

## TIDAL EFFECTS ON SOURCE INVERSION

MICHAEL B. PORTER

*Ocean Sciences Division  
Science Applications International Corporation  
10260 Campus Point Drive  
San Diego, CA 92121-1578, USA*

SERGIO M. JESUS

*UCEH, Universidade do Algarve  
8000 Faro, PORTUGAL*

YANN STÉPHAN, XAVIER DÉMOULIN

*Centre Militaire d'Océanographie  
EPSHOM, BP426  
29275 Brest Cedex, FRANCE*

EMANUEL COELHO

*Instituto Hidrographico  
Ruas das Trinas 49  
1296 Lisbon, PORTUGAL*

### Abstract

In the summer of 1996, an experiment was conducted off the coast of Portugal to study the effects of internal tides on sound propagation. This experiment—called INTIMATE '96 (Internal Tide Investigation by Means of Acoustic Tomography Experiment)—has provided a great deal of insight about the variability of pulse transmission over space and time. In contrast to a common view of shallow-water propagation as complicated and unpredictable, we find a steady pattern of echoes. The echo-pattern stretches and shrinks in a systematic way with the tides and allows us to infer the components of the first few oceanographic modes. We also used the echo-pattern to track the source over a period of several days. During this period the isotherms in the ocean wavered by 20 m as a result of the tides, providing a challenge for model-based tracking. We will discuss these acoustic results with emphasis on the source tracking.

### 1. Introduction

Tidal effects have been observed for many years in ocean acoustics [1,2,3,4,6,7]. To better understand their role, an experiment INTIMATE96 (Internal Tide Monitoring by means of an Acoustic Tomography Experiment) was conducted off the Portuguese coast. In effect, a sequence of impulses was sent over a period of several days providing a probe of the channel. The goal of the experiment was to study the inverse problems for both the ocean structure and the source position.

The oceanographic inversion is described in a companion paper [10]. Briefly summarizing those results, the tidal forces excite internal waves (which are then called internal tides). The internal tides form an infinite set of space- and time-varying oceanographic modes. The first of these is the barotropic mode, which is simply the familiar tide. Each of these modes has a different effect on the acoustic arrival pattern. Thus the coefficients associated with these modes can be derived yielding an acoustically-derived image of the ocean temperature structure.

One of the reasons for being interested in the tides is to understand how they affect another inverse problem: that of inferring the source location in the waveguide. This type of problem arises in a variety of areas. For instance, we can learn a lot about the behavior of marine mammals such as whales by using their own sounds to track them. Similarly it is often useful to be able to accurately determine the range and/or depth of underwater vehicles.

There has now been a great deal of work in source-localization motivated by the naval application. A readable summary of the work up to 1991 is given by Tolstoy [11]. Until recently this work has been predominantly focused on tones; however, more recently broadband signals have become of interest and these will be the focus of our attention. Our goal is to both devise robust localization-algorithms and understand the impact of the tides on their performance.

## 2. Experimental Scenario

As the experiment has been discussed in detail in [10] we will be brief. A site was selected off the Portuguese coast in an area where strong internal tide activity was expected (see Figure 1). The experiment was divided into three phases as shown in Figure 2: 1) a 25-hour station with the source located about 6 km north of the vertical receiving-array, 2) a tracking test in which the source was towed over a sort of bowtie pattern around the array, 3) another 25-hour station with the source located about 6 km west of the vertical receiving array. These will be referred to as the “*North Station*”, “*Tracking*”, and “*West Station*” phases respectively.

The various phases were motivated by separate needs for the tomographic and localization aspects of the program. The North Station was specifically chosen to be range-independent in terms of both the ocean sound-speed structure and the landscape of the ocean bottom. This provided a more benign environment for understanding the propagation conditions and validating the tracking. (Note however that while the spatial variation was small, the temporal variation due to the tides was strong.)

## TIDAL EFFECTS ON SOURCE INVERSION

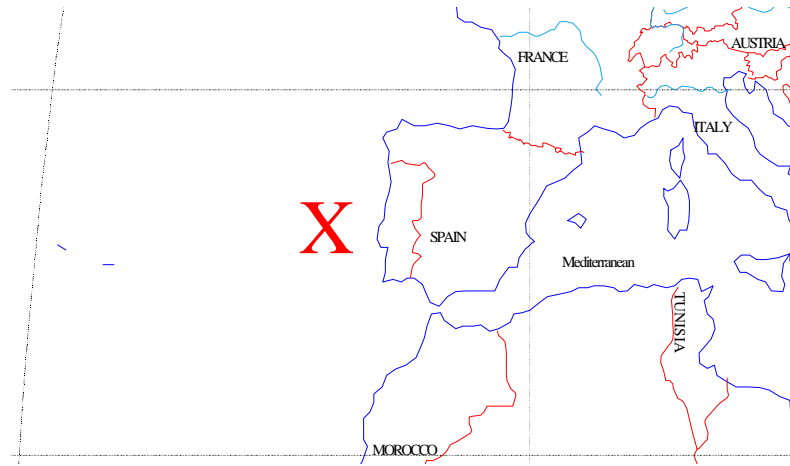


Figure 1. Location of the INTIMATE96 experiment.

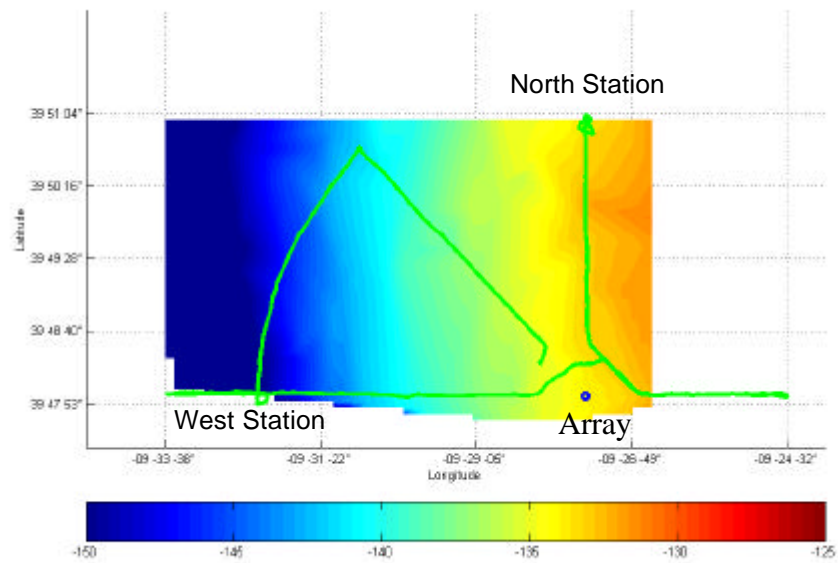


Figure 2. Source track (thick green line) relative to the bottom topography.

The Tracking Phase was chosen to provide a convincing demonstration of the localization over both time and space. One of the key limitations of past localization work has been limited amount of data processed. Typically a few snapshots are presented or tracking results over periods of at most an hour. Here we sought to track the source over a long time period (a day) and over a sweep of source ranges. In addition, we scheduled a fan of different bearing-lines passing over both range-independent and range-dependent sections.

Finally, the West Station was chosen in a direction slicing through both the wavefronts of the internal tides and in the direction of the topographic gradient thus giving the greatest range variation.

### 3. Broadband Source-Localization

There are several points of view one can take in constructing broadband localizers. The literature is now quite large but a useful introduction is given in references [11-22].

The *matched-field processing* view uses array processing ideas but replaces conventional planewave steering vectors with replica vectors that take into account the refractive and multipath effects of the ocean channel [11].

*Time-reversal* (a.k.a., back-propagation or phase-conjugation) takes the view that if we simulate the acoustic field that arises when the received waveform is re-transmitted from each of the receivers then that field will have a peak in mean intensity at the source position (see [17] and references therein).

*Correlation-tracking* takes the view that the auto-correlation for the waveform on a single phone (or the cross-correlation between two phones) yields a sequence of impulses that is a unique signature of the source position [19]. Thus, that signature can be compared to an ensemble of predicted signatures corresponding to different source positions to find the best match and thereby the source position.

Although these three perspectives sound quite different, identical processors can be derived from each. The strengths and weaknesses assigned to each scheme are then often the result of a superficial analysis. On the other hand, certain improvements in the localization methods are often easier to derive from one or the other perspective and the resulting approach may then be difficult to derive or interpret in another framework.

The approach taken here is based on correlograms and assumes initially a known source spectrum. The case of known-spectrum is important itself but later on we shall discuss the modifications required when the spectrum is not known. The first stage is then to correlate the received waveform with a replica of the source waveform:

$$rr(t) = \int r(\mathbf{t} - t)s(\mathbf{t})d\mathbf{t} . \quad (1)$$

The resulting function,  $rr(t)$ , is referred to as the *replica-correlogram*. Replica correlation is also the usual first stage in ocean acoustic tomography. To understand the result it is useful to take a ray-theoretic view of the channel. Neglecting phase changes, the received waveform is a sum of delayed and scaled versions of the source waveform:

$$r(t) = \sum A_i s(t - t_i) . \quad (2)$$

Replica correlation then yields

$$rr(t) = \int \sum A_i s(\mathbf{t} - t + t_i) s(\mathbf{t}) d\mathbf{t} = \sum A_i ss(t - t_i), \quad (3)$$

where,  $ss(t)$ , is the auto-correlation function of the source:

$$ss(t) = \int s(\mathbf{t} - t) s(\mathbf{t}) d\mathbf{t}. \quad (4)$$

The goal of this process is to produce a waveform,  $rr(t)$ , with robust features for localization. In particular, one often seeks to make  $ss(t)$  a sharp function like the delta-function. Then the replica-correlogram looks like the channel impulse-response with peaks matching the strengths and delays of the echoes in the channel.

Any source waveform that has a flat spectrum will have a sinc-pulse as its autocorrelation function and will therefore have a peak. Linear FM chirps, pseudo-random noise, and m-sequences are all reasonable choices with sharply peaked auto-correlations. Certain FM chirps have the property that they are Doppler insensitive which is attractive for moving sources. On the other hand, if the chirp length is chosen too long, they cannot be processed in segments without reducing temporal resolution. In acoustic tomography, m-sequences have historically been used. They are easy to implement in hardware; however, this does not seem to be an issue with today's fast processors.

In a correlator-tracker we invert for the source position by comparing the measured impulse-response,  $rr(t)$ , to an ensemble of modeled versions,  $hh(t; r_s, z_s)$ , seeking the source coordinate,  $(r_s, z_s)$  that gives the best match between model and data. The way in which we measure the match can be important. In tomographic applications this is typically done using only the arrival times and minimizing the mean-square error between the arrival times in the model and data. This process is fine for a scientific environment but is difficult to automate, especially at low SNR. A reasonable alternative is simply to correlate model and data:

$$C(t; r_s, z_s) = \int rr(t - \mathbf{t}) hh(\mathbf{t}; r_s, z_s) d\mathbf{t}. \quad (5)$$

At this point there is an important choice to make. We can look for either the peak in  $C(t; r_s, z_s)$ , or its overall power. If we look for a peak we have a sort of coherent processor that allows localization with a single phone. If we use the total power we have an incoherent processor. Furthermore since Parseval's Theorem assures us that the power calculated in the frequency domain is the same as that in the time domain, the multi-phone correlator tracker becomes equivalent to the matched-field processing averaged incoherently across frequency.

#### 4. Log-envelope Correlation Tracker

As discussed above, the echo-pattern—besides being a useful signature of the environment for tomography—is also a signature of the source position. The problem is that environmental uncertainty prevents the acoustic models from providing precise predictions of the echo pattern. This so-called environmental mismatch has typically been identified as a key issue in applying model-based localization schemes.

To capture the robust features for source localization, we modify the correlation tracker in two ways. First, instead of comparing modeled and received replica-

correlograms we compare the *envelopes* of each. The envelope is insensitive to pulse-inversions that occur when the sound reflects from the ocean surface. More importantly, it is also insensitive to the more complicated phase changes that occur during bottom reflection. If the bottom were precisely known, those phase changes would be extra useful information in localizing a source. However, this is not the case so the uncertainty just makes it hard to match model and data and degrades the performance.

Secondly, after forming the envelopes we take a logarithm before doing the correlation between model and data. This modification was motivated by the data. It was seen that the overall echo-pattern provided an immediate visual indication of the source but that a direct model-data correlation did not provide reasonable localizations. The data showed that most of the energy was contained in a few early arrivals that were not separated in time and interfered with each other in a way that was difficult to predict. Thus, direct correlation is energetically dominated by a portion of the waveform that is poorly predicted. Taking the logarithm of the envelope brings into balance the weak and strong arrivals (and diminishes the sensitivity to the amplitude of each echo). The result then is a localization algorithm that is sensitive mainly to the arrival times in the echo-pattern and not their strengths. Meanwhile, it eliminates the peak-picking procedure used in acoustic tomography.

To summarize, for each normalized measured and modeled time series,  $rr(t)$  and  $hh(t; r_s, z_s)$  respectively, we compute in sequence:

$$\begin{aligned} r_{le}(t) &= 20\log[\text{env}(rr(t))] - a, \\ h_{le}(t) &= 20\log[\text{env}(hh(t; r_s, z_s))] - a, \\ C(t; r_s, z_s) &= \int r_{le}(\mathbf{t})h_{le}(\mathbf{t} - t; r_s, z_s)d\mathbf{t}, \\ P(r_s, z_s) &= \max_t |C(t; r_s, z_s)|. \end{aligned} \tag{6}$$

Here  $a$  is set at 30 dB to clip out the noise that would otherwise dominate the correlation. For efficiency the correlation is implemented in the frequency domain. In an obvious generalization, information from multiple phones can be included by summing cross-correlations between phones (cross-correlation tracker); however, here we present only results using the deepest phone. In theory, the resulting ambiguity surface,  $P(r_s, z_s)$  then has a peak at the source location.

Note that this processing assumes that the replica-correlogram,  $rr(t)$ , is available and this in turn assumes a knowledge of the source spectrum. In many important applications this is known. When it is not, one may correlate the autocorrelations of each phone with predicted autocorrelations with much weaker assumptions needed about the source spectrum. Also, if the auto-correlation of the source does not show a strong peak this can often be corrected by pre-whitening.

## 5. Acoustic Modeling

A common ingredient in all of these localization schemes is the use of an acoustic model of the channel. Fortunately, ocean channel-models are now well-developed and there are many suitable choices [25]. In this work we have used several models including the SCOOTER wavenumber-integration model; the KRAKEN normal-

## TIDAL EFFECTS ON SOURCE INVERSION

mode program[26]; and the BELLHOP ray/beam model. The BELLHOP model is probably the least accurate but is also the fastest and most convenient for these broadband, range-dependent problems. As we will see later the channel is characterized by a number of distinct multipaths associated with surface and bottom echoes. There is little concern about the accuracy for these paths.

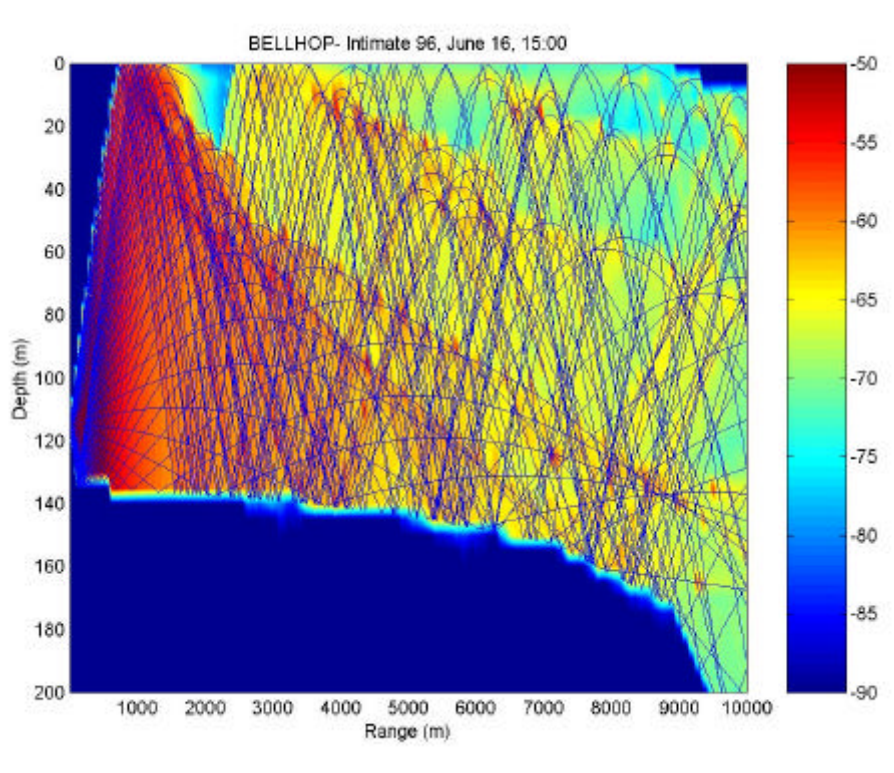


Figure 3. Ray paths superimposed on transmission loss.

Figure 3 shows a BELLHOP prediction of the ray paths propagating in the down-slope direction from the lowest phone on the vertical array. The ray picture has been superimposed on a transmission loss plot for a 500 Hz central frequency. The models are generally designed to propagate from a fixed source to multiple receiver ranges. Thus, we invoke the reciprocity principle that the received time series is the same when source and receiver position are exchanged.

The ray picture indicates that the sound speed profile is downward-refracting with the paths having the shallowest angles refracting before hitting the surface. The steeper paths hit both the surface and the bottom.

## 6. Experimental Demonstration

### 6.1 NORTH STATION

Acoustic data was collected during the experiment on a 4-phone vertical line array with phones at 35, 70, 105 and 115 m in depth. The echo-pattern seen by the deep-

est phone over the 25-hours of the North Station is shown in Figure 4. As described above, this pattern is obtained by replica-correlation, that is, by correlating the received waveform with a replica of the transmitted waveform and then forming the log of the envelope. We have also aligned the data by a ‘leading edge’ defined by the point where the envelope reaches 90% of its peak value. This eliminates a large part of the variation caused by fluctuations in the mean arrival time.

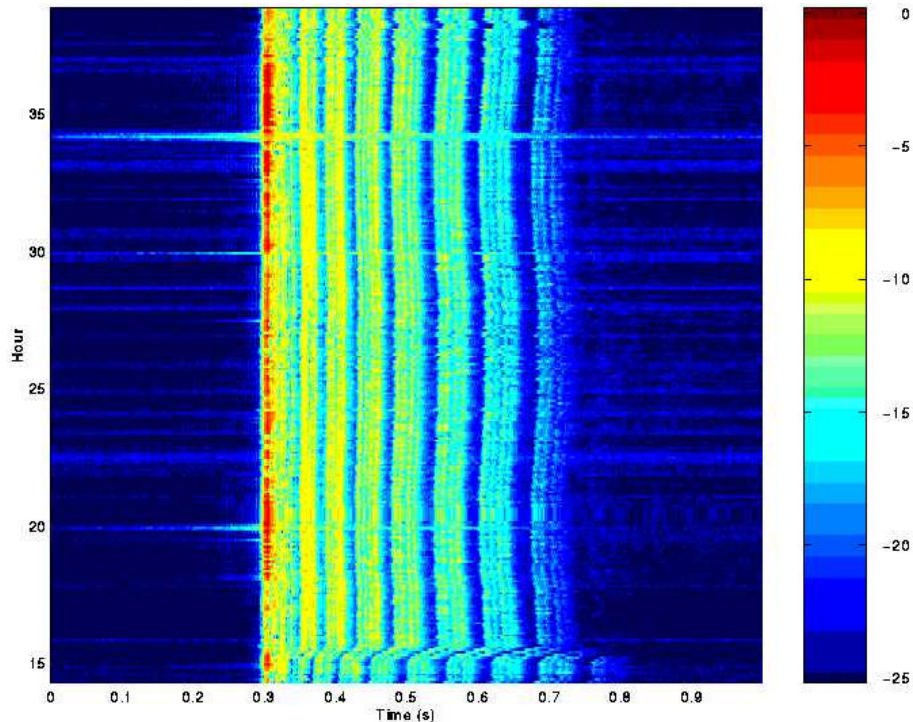


Figure 4. Replica-correlogram for the North station.

We can see a distinct pattern of echoes clustered in groups of 4 representing additional bottom and surface reflections. (The shift during the first 30 minutes is a period where the ship was moving onto station.) The other obvious feature is the sinusoidal modulation of the arrivals. This is clearest on the latest arrivals where we see that the arrival time fluctuates by about 10 ms in synchronization with the barotropic tide. (These tidal influences are discussed in greater detail in the companion paper[10]).

In a qualitative sense we would characterize these results as extremely stable: The general characteristics of the pattern are unchanged over the 25-hours of the station. However, if we look at a single frequency-component we would see that this stretching and shrinking of the echo-pattern by the tides causes individual components to move rapidly in the complex plane. Similarly, if we use a conventional beamformer that is sensitive to the overall power, it will be dominated by the leading portion of the time-series (that contains most of the energy). It also is seen to vary significantly and is therefore not an effective feature on which to base the localization.

The range-time ambiguity surface using the log-envelope processor is shown in Figure 5. Note that the log-envelope processor provides an unambiguous

## TIDAL EFFECTS ON SOURCE INVERSION

localization in range for the entire 25-hour period. It is also interesting that there is a sort of mirage due to the tides that causes the apparent source range to vary in synchronization with the tide. (The source was at a fixed range of about 5.7 km.) These results are to our knowledge by far the longest demonstration of model-based tracking. It is also of note that these results were obtained using a single, static measurement of the ocean sound-speed profile while the ocean was obviously quite dynamic. Since the ocean SSP was regularly measured and since accurate tidal information was available the mirage could have been corrected. However, it is a great advantage that the processor functions reliably without this more detailed environmental information.

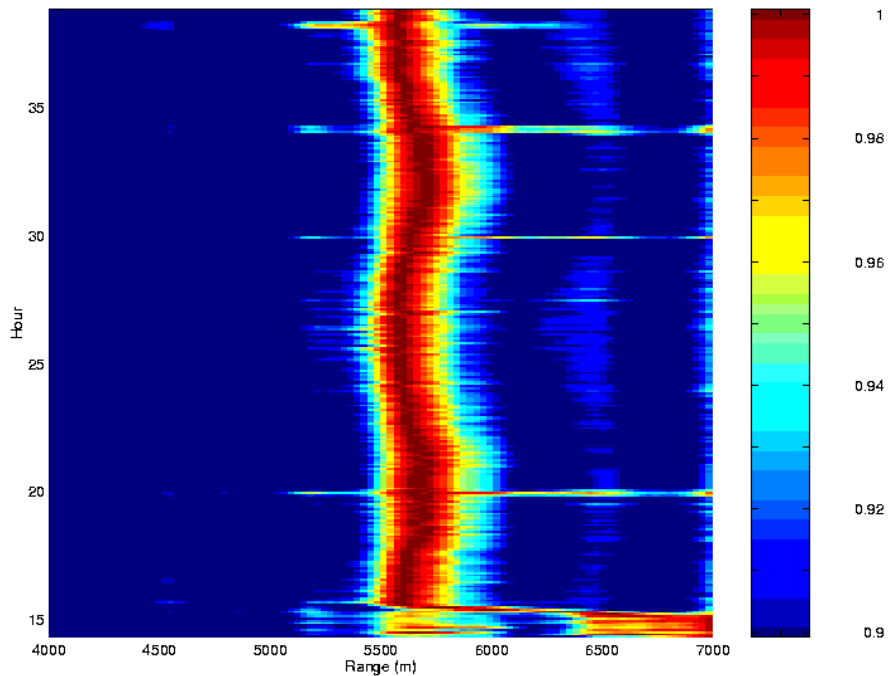


Figure 5. Range-time track for the North station.

### 6.2 TRACKING PHASE

The second phase presented a much more serious challenge since, as discussed above, we have significant variation in the bottom topography and we are also slicing through a range-dependent sound-speed profile. In addition, the variation in range means that one cannot tune the processor to function well at a single range as has often been done in MFP work.

Turning first to the basic acoustic data in Figure 6, we see that once again the echo pattern is, in a sense, very stable. The multipath-spread varies significantly over the complicated track but it expands and contracts in a systematic way in proportion to the source range. As before, we see a characteristic pattern involving clusters of 4 arrivals associated with the various surface and bottom echoes. With the aid of an acoustic model we can also clearly see how the delays within that cluster provide a unique fingerprint of the source depth.

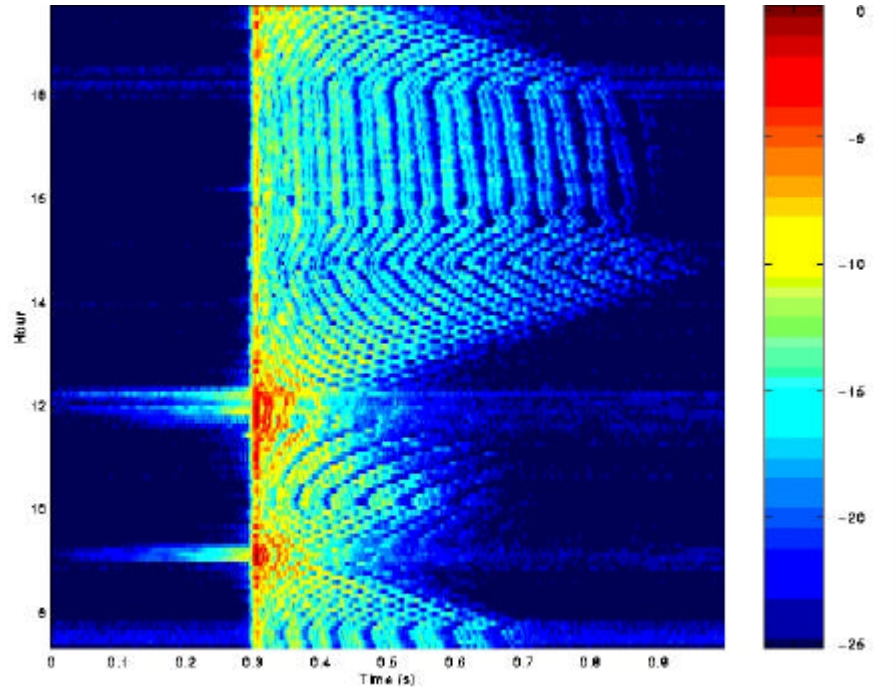
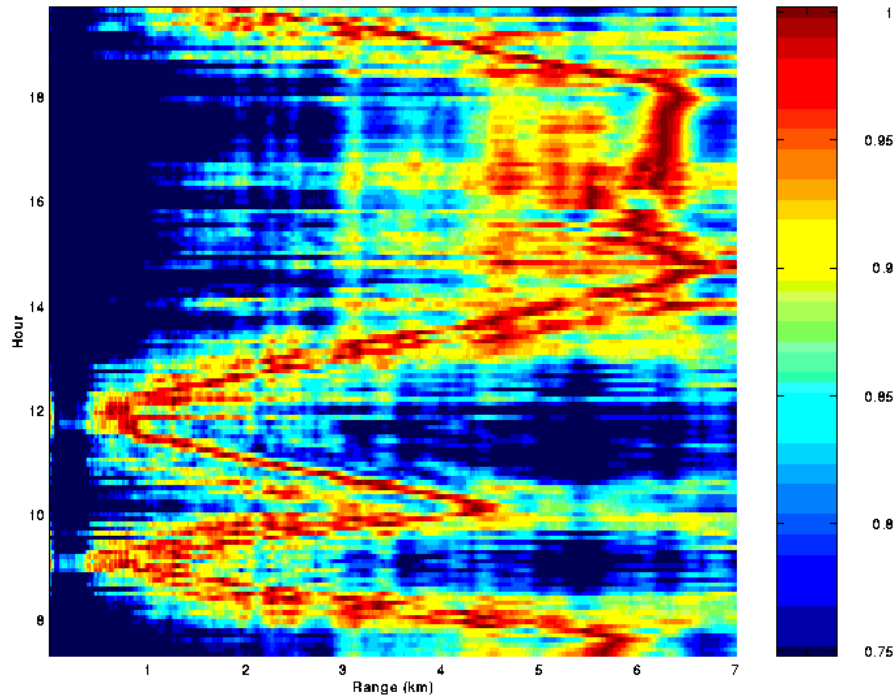


Figure 6. Replica-correlogram for the tracking phase.

The behavior of the multipath-spread is of particular importance in acoustic communications since it determines the channel clearing times for simple incoherent schemes or the number of taps in adaptive equalizers. It is worth noting that the echo pattern can vary widely with the environment and in some cases the multipath spread can actually drop significantly at certain ranges. Note also that when the source is very close there is a strong arrival refracted in the sediment causing the precursors at about 9:30 and noon.

The results of applying the log-envelope processor to the data are shown in Figure 7. Note that the processor tracks the source very clearly throughout most of the 16 hours of data available.

## TIDAL EFFECTS ON SOURCE INVERSION



*Figure 7.* Range-time record for the tracking phase.

Comparing to an independent reference for the source range, we see that there is a bias during the period from about 14:00 to 16:00 when the source is in the down-slope region. This also corresponds to the period where the sidelobes are highest. As before, we have used a static and range-independent model to do the tracking. The success of the results speaks to the robustness of the processing. These results could be improved still further with a range-dependent calculation.

Finally, we show the depth-time record in Figure 8. The super-imposed black-line is an independent measurement from a pressure sensor on the source. Again the algorithm tracks the source position accurately over most of the 16-hour period. The down-slope period again shows the greatest sidelobes reflecting the errors in using a flat-bottom model in a range-dependent environment.

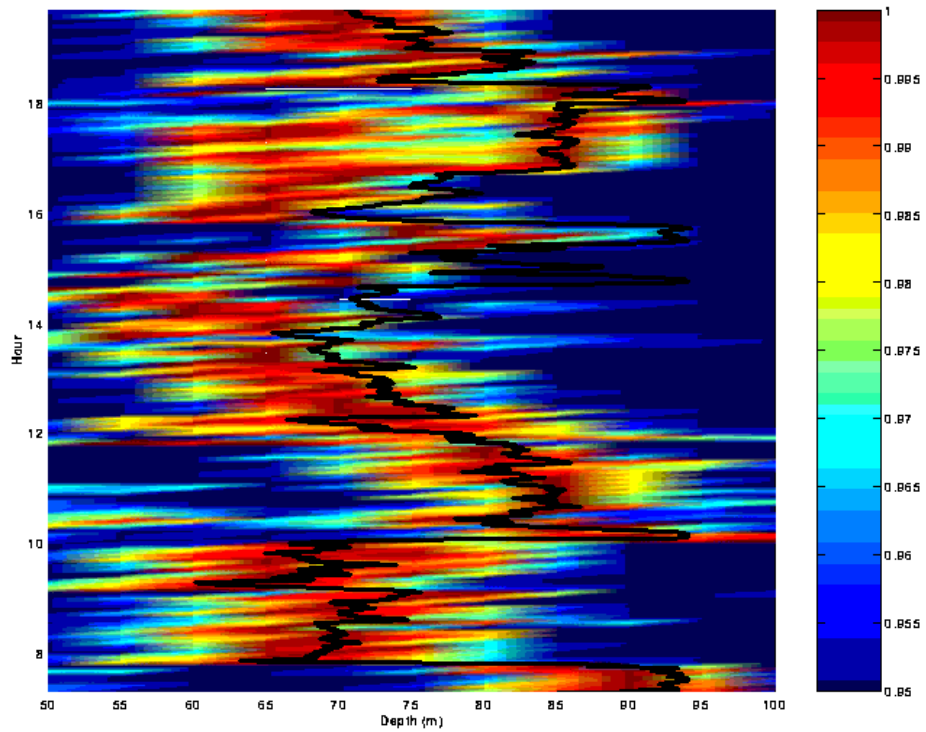


Figure 8. Depth-time record for the tracking phase.

### 6.3 WEST STATION

The West Station is significantly harder than the North Station since it lies on a range-dependent track passing over the continental slope. In addition, the oceanography showed an even stronger effect due to tides. However, once again the acoustic data (Figure 9) shows a regular pattern of expanding and contracting multipath spread again under the influence of the tides.

## TIDAL EFFECTS ON SOURCE INVERSION

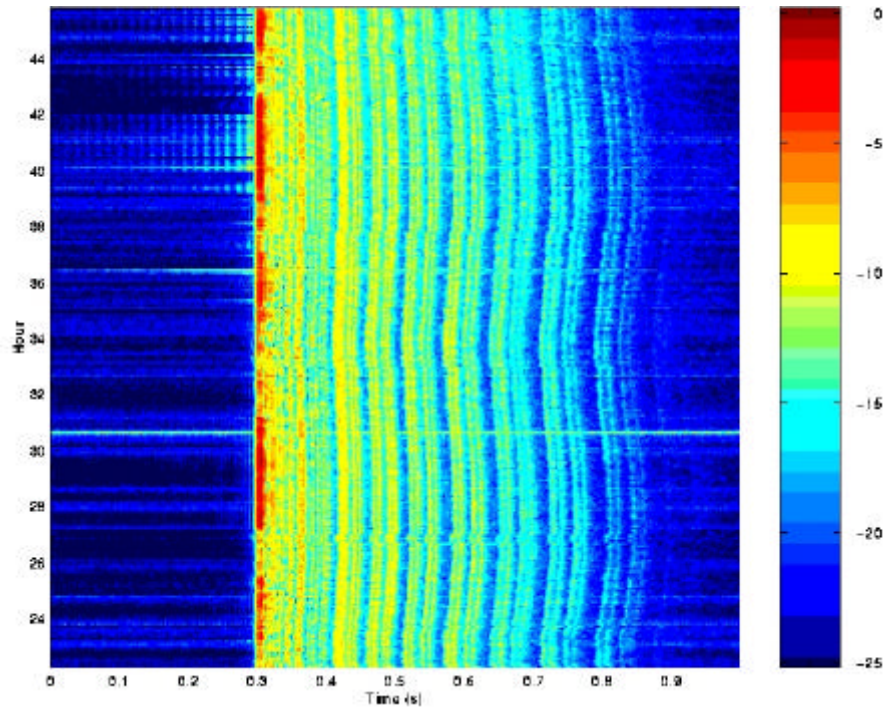


Figure 9. Replica-correlogram for the West station.

The results of the log-envelope processor to localize the source are shown in Figure 10. The processor again provides a clear and stable estimate of the 6.7 km source range for the entire 25-hours of this third phase of the experiment. Here we should note that it was necessary for the first time to include the bathymetry to obtain a clear localization. It was also necessary to take an updated measurement of the sound-speed profile; however, no attempt was made to account for the ocean dynamics. This explains the mirage causing the source to appear to meander in range even though it is fixed.

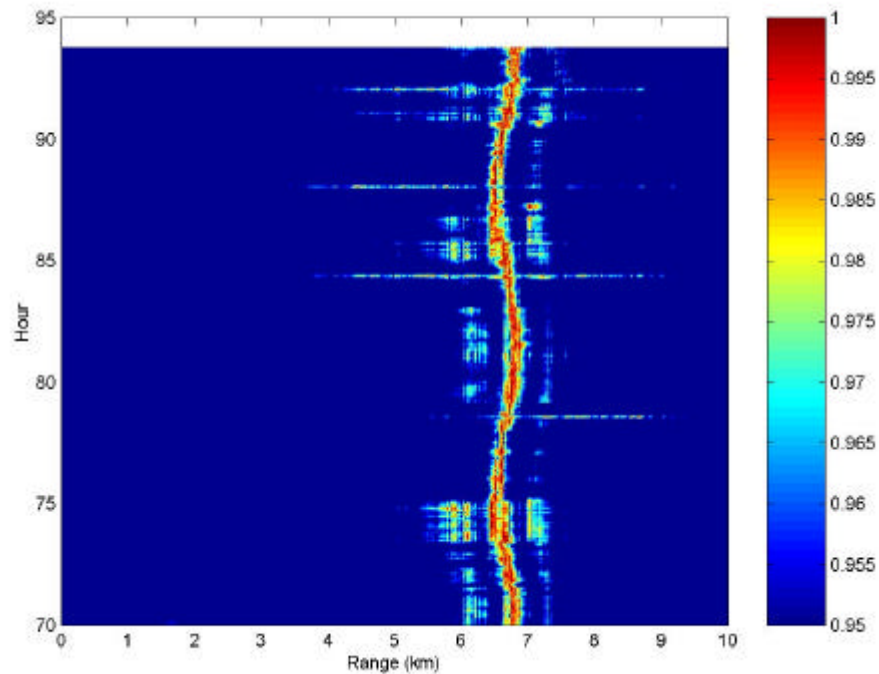


Figure 10. Range-time record for the West station.

The depth-time ambiguity surface is shown in Figure 11 and provides another indication of the validity of the process. We see a peak at the correct depth of 90 m with an uncertainty of perhaps plus or minus 5 m and with occasional errors of up to 15 m. Comparing the range-time and depth-time surfaces we see that when the sidelobes in range are high, the sidelobes in depth are also high. The sidelobes of the range plot most likely reflect the difficulty of distinguishing between echo patterns with one fewer or one additional cluster of 4 echoes.

## TIDAL EFFECTS ON SOURCE INVERSION

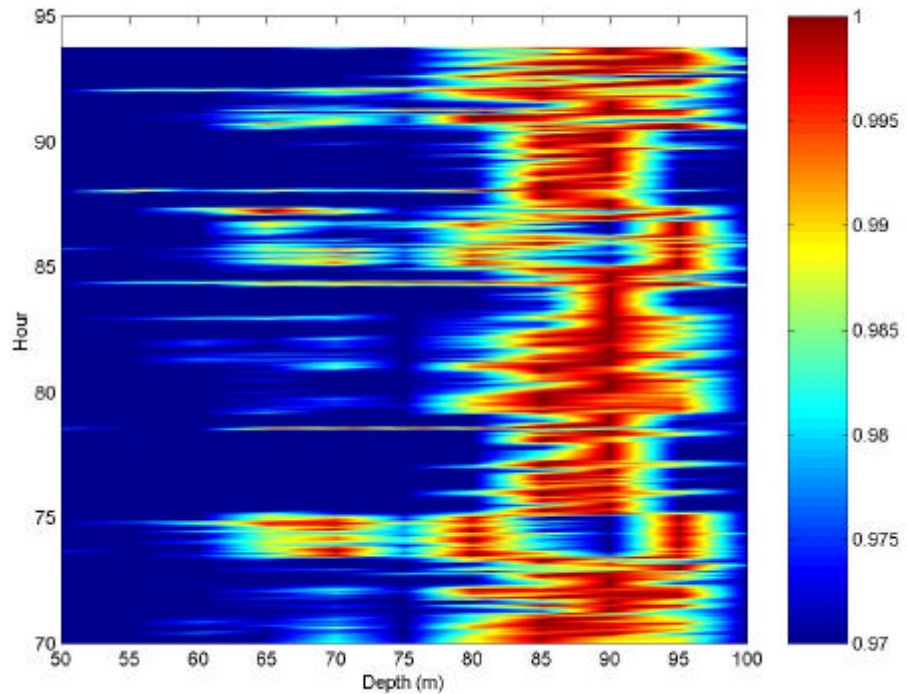


Figure 11. Depth-time record for the West station.

### 7. Summary and Conclusions

Model-based localization is potentially of great value. Alternatives based on target-motion analysis and planewave beamforming are much slower and do not provide depth discrimination.

The log-envelope processor has been seen to be very robust with respect to mismatch. The results presented here demonstrate the model-based tracking over periods that are at least an order of magnitude (several days) longer than previous results. The processor is sufficiently robust that we have been able to eliminate the simultaneous environmental inversion used in previous work[18].

There are two key challenges for the future. First, the performance under low SNR is yet to be clearly quantified. Clearly the algorithm relies on a pattern of echoes to do the localization and these must be seen above a noise background. All model-based algorithms rely on the visibility of this sort of fingerprint (manifested spatially or temporally) for source localization. We can say that the algorithm was also successful on a very low SNR phone that failed during the experiment.

Secondly, the algorithm currently assumes some knowledge about the source spectrum. This is an important scenario, however, we envision the general algorithm as functioning based on cross-correlations between phones in an array or auto-correlations for single-phone localization for a source whose spectrum is less well known. Future work will address both these issues.

The tides play a central role in this work and it is clear that without dynamic compensation they induce a sort of mirage causing the source to appear to wander in range on a tidal cycle. For the applications we consider, this is not a serious issue.

### Acknowledgments

This work was supported in part by ONR Grant N00014-95-0558. One of us (M.B.P) gratefully acknowledges support under the PRAXIS program as a visiting Professor at the Universidade do Algarve and under the sabbatical program of the New Jersey Institute of Technology. The data was collected on a portable array lent to us by the SACLANT Undersea Research Centre.

### References

1. B.D. Dushaw, B.D. Cornuelle, P.F. Worcester, B.M. Howe, and D.S. Luther, "Barotropic and baroclinic tides in the central North Pacific Ocean determined from long-range reciprocal acoustic transmission", *J. Phys. Oceanography*, **25**(4) 631-647 (1995).
2. F.R. Martin-Lauzer, Y. Stéphan, and F. Evennou, "Analysis of tomographic signals to retrieve tidal parameters", *Proceedings of the Second European Conference on Underwater Acoustics*, Ed. L. BjørnØ, European Commission, 1051-1056 (1994).
3. W. Munk and C. Wunsch, "The Moon, of course ...", *Oceanography*, **10**, No. 3 (1997).
4. W. Munk, B. Zetler, J. Clark, S. Gill, D. Porter, J. Spiesberger, and R. Spindel, "Tidal effects on long-range sound transmission", *J. Geophys. Research*, **86**(C7), 6399-6410 (1981).
5. Open University Course Team, *Waves, Tides, and Shallow-Water Processes*, Open University press (1989).
6. N.L. Weinberg, J.G. Clark, and R.P. Flanagan, "Internal tidal influence on deep-ocean acoustic ray propagation", *J. Acoust. Soc. Amer.*, **56**(2), 447-458 (1974).
7. M. Badiey, "Frequency dependence of broadband propagation in coastal regions", *J. Acoust. Soc. Amer.*, **101**(6):3361-3370 (1997).
8. M. Porter, S. Jesus, Y. Stéphan and X. Démoulin, E. Coelho, "Exploiting reliable features of the ocean channel response", *Shallow Water Acoustics*, R. Zhang and J. Zhou, Eds., China Ocean Press, p. 77-82, Beijing, China (1998).
9. X. Démoulin, Y. Stéphan, S. Jesus, E. Coelho, and M. Porter, "INTIMATE96: A shallow-water tomography experiment devoted to the study of internal tides", *Shallow Water Acoustics*, R. Zhang and J. Zhou, Eds., China Ocean Press, p. 485-490, Beijing, China (1998).
10. Y. Stéphan, X. Démoulin, T. Folégot, S.M. Jesus, M.B. Porter, E. Coelho, "Acoustic effects of internal tides on shallow water propagation: An overview of the INTIMATE96 experiment", *Experimental Acoustic Inversion Methods*, Eds. A. Caiti, S. Jesus, J-P. Hermand, M.B. Porter, Kluwer (2000).
11. A. Tolstoy, *Matched-Field Processing for Underwater Acoustics*, World Scientific, Singapore (1993).
12. A.B. Baggeroer, W.A. Kuperman, P.N. Mikhalevsky, "An overview of matched-field methods in ocean acoustics", *IEEE J. Oceanic Eng.* **OE-18**(4):401-424 (1993).
13. J.P. Ianniello, "Recent developments in SONAR signal processing", *IEEE Signal Processing Magazine*, **15**(4):27-40 (1998).
14. R.K. Brienza and W.S. Hodgkiss, "Broadband matched-field processing", *J. Acoust. Soc. Amer.*, **94**(5), 2821-2831 (1993).
15. Evan K. Westwood, "Broadband matched-field source localization", *J. Acoust. Soc. Amer.*, **91**(5):2777-2789 (1992).
16. Evan K. Westwood and David P. Knobles, "Source track localization via multipath correlation matching", *J. Acoust. Soc. Amer.*, **102**(5), 2645-54 (1997).
17. Michael B. Porter, "Acoustic Models and Sonar Systems," *IEEE J. of Oceanic Engineering*, Vol. OE-18(4):425-437 (1994).
18. Z.H. Michalopoulou, M.B. Porter, and J. Ianniello, "Broadband source localization in the Gulf of Mexico", *Journal of Computational Acoustics*, **2**(3),361-370 (1996).
19. William S. Burdic, *Underwater Acoustic System Analysis*, 438-441, Prentice Hall, Englewood Cliffs (1991).
20. Newell O. Booth, Paul A. Baxley, Joseph A. Rice, Phil W. Schey, Willaims S. Hodgkiss, Gerald L. D'Spain, and James Murray, "Source localization with broad-band matched-field processing in shallow water", *IEEE J. Oceanic Eng.*, **21**(4), 402-412 (1996).
21. G.L. D'Spain, J.J. Murray, W.S. Hodgkiss, N.O. Booth, P.W. Schey, "Mirages in shallow-water matched-field processing", *J. Acoust. Soc. Amer.*, **105**(6), 3245-3265 (1999).

## TIDAL EFFECTS ON SOURCE INVERSION

22. C.S. Clay, "Optimum time-domain signal transmission and source location in a waveguide", *J. Acoustic. Soc. Amer.*, **81**(3):660-664 (1987).
23. S.M. Jesus, "Broadband matched-field processing of transient signals in shallow water", *J. Acoust. Soc. Amer.*, **93**(4):1841-1850 (1993).
24. L.N. Frazer and P.I. Pecholcs, "Single-hydrophone localization", *J. Acoust. Soc. Amer.*, **88**, 995-1002 (1990).
25. F. Jensen, W. Kuperman, M. Porter and H. Schmidt, *Computational Ocean Acoustics*, Springer-Verlag, (2000).
26. M. B. Porter, *The KRAKEN normal mode program*, SACLANT Undersea Research Centre Memorandum (SM-245) / Naval Research Laboratory Mem. Rep. 6920 (1991).